ResearchGate

See discussions, stats, and author profiles for this publication at: https://www.researchgate.net/publication/343198810

Beam Illumination Pattern Design in Satellite Networks: Learning and Optimization for Efficient Beam Hopping

Article *in* IEEE Access · July 2020

DOI: 10.1109/ACCESS.2020.3011746

CITATIONS
0

READS
37

6 authors, including:

Lei Lei
University of Luxembourg
62 PUBLICATIONS **817** CITATIONS
SEE PROFILE

Yaxiong Yuan
University of Luxembourg
11 PUBLICATIONS **20** CITATIONS
SEE PROFILE

Mirza Kibria
University of Luxembourg
43 PUBLICATIONS **244** CITATIONS
SEE PROFILE

Symeon Chatzinotas
University of Luxembourg
433 PUBLICATIONS **5,213** CITATIONS
SEE PROFILE

Some of the authors of this publication are also working on these related projects:

ProCAST: Proactive Edge CAching for Content Delivery Networks powered by Hybrid Satellite/Terrestrial Backhauling View project

Multiagent Communications Over Imperfect Chennels View project

All content following this page was uploaded by Yaxiong Yuan on 27 July 2020.

The user has requested enhancement of the downloaded file.

This article has been accepted for publication in a future issue of this journal, but has not been fully edited. Content may change prior to final publication. Citation information: DOI 10.1109/ACCESS.2020.3011746, IEEE Access

IEEE Access
Multidisciplinary | Rapid Review | Open Access Journal

Date of publication xxxx 00, 0000, date of current version xxxx 00, 0000.

Digital Object Identifier xx.xxxx/ACCESS.xxxx.DOI

Beam Illumination Pattern Design in Satellite Networks: Learning and Optimization for Efficient Beam Hopping

LEI LEI **(Member, IEEE)**, EVA LAGUNAS **(Senior Member, IEEE)**, YAXIONG YUAN **(Student Member, IEEE)**, MIRZA GOLAM KIBRIA **(Member, IEEE)**, SYMEON CHATZINOTAS **(Senior Member, IEEE)**, and BJÖRN OTTERSTEN **(Fellow, IEEE)**
Interdisciplinary Centre for Security, Reliability and Trust, Luxembourg University, Luxembourg

Corresponding author: Lei Lei (e-mail: lei.lei@uni.lu).

This work was supported in part by the European Research Council (ERC) project AGNOSTIC (under grant 742648), the FNR CORE project ROSETTA (under grant 11632107), the FNR CORE project FlexSAT (under grant 13696663), and the ESA project SATNEX IV (Opinions, interpretations, recommendations and conclusions presented in this paper are those of the authors and are not necessarily endorsed by the European Space Agency).

ABSTRACT

Beam hopping (BH) is considered to provide a high level of flexibility to manage irregular and time-varying traffic requests in future multi-beam satellite systems. In BH optimization, adopting conventional iterative heuristics may have their own limitations in providing timely solutions, and directly using data-driven technique to approximate optimization variables may lead to constraint violation and degraded performance. In this paper, we explore a combined learning-and-optimization (L&O) approach to provide an efficient, feasible, and near-optimal solution. The investigations are from the following aspects: 1) Integration of BH optimization and learning techniques; 2) Features to be learned in BH design; 3) How to address the feasibility issue incurred by machine learning. We provide numerical results and analysis to show that the learning component in L&O significantly accelerates the procedure of identifying promising BH patterns, resulting in reduced computing time from seconds/minutes to milliseconds level. The identified learning feature enables high accuracy in predictions. In addition, the optimization component in L&O guarantees the solution's feasibility and improves the overall performance with around 5% gap to the optimum.

INDEX TERMS Beam hopping, machine learning, neural network, optimization, satellite communications.

I. INTRODUCTION

Data-driven techniques have been widely studied in terrestrial wireless communications fields, proving the benefits and potentials of such techniques [1]–[3]. Among the several applications analyzed in the terrestrial domain, solving the large-scale resource management optimization problems is one of the areas where learning techniques can bring significant benefits. Optimization problems associated with frequency and power allocation, spectrum management, power control, intelligent beamforming are a few examples that are of high relevance to satellite communications (Satcom) systems. The application of data-driven techniques for satellite networks are studied to a limited extent in the literature. The latter motivates this paper to investigate learning-based solutions to optimize the satellite resource allocation in multi-beam system scenarios with non-uniform traffic demands. In the following, we explain the concept of beam hopping (BH), state-of-the-art, and the contribution of this paper.

A. FLEXIBLE SATELLITE ENABLER: BEAM HOPPING

Satellite resources are expensive and thus it is necessary to optimize and, whenever possible, time-share these precious resources. The capability to flexibly allocate on-board resources over the service coverage area is becoming a must for future broadband multibeam satellites. Previous and current systems have shown that in large multibeam satellites the demand in some spot beams greatly exceeds the available capacity (hot–spots) while in others the situation is inverted (cold–spots). This raises a paradoxical scenario where demand is left unmet in the hot–spots while capacity is left

This work is licensed under a Creative Commons Attribution 4.0 License. For more information, see https://creativecommons.org/licenses/by/4.0/.

This article has been accepted for publication in a future issue of this journal, but has not been fully edited. Content may change prior to final publication. Citation information: DOI 10.1109/ACCESS.2020.3011746, IEEE Access

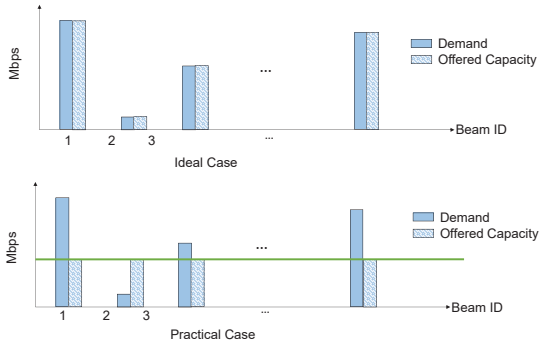

Figure 1. Offered and requested capacity in ideal and practical scenarios.

unused in the cold–spots. The consequence for the satellite operator and service provider is twofold: (i) a loss of the revenue corresponding to the unmet demand plus, (ii) the loss of the investment in the unused capacity. The primary goal of flexibility is then to solve this paradox and maximize the amount of system capacity that is actually used (or sold) by allocating it where needed. In conventional payloads, the resources per beam are fixed and uniformly distributed across beams [4], therefore providing the same capacity to each beam, e.g., Fig. 1, down-side. In this work, we aim to assign the resources according to the asymmetric traffic demands.

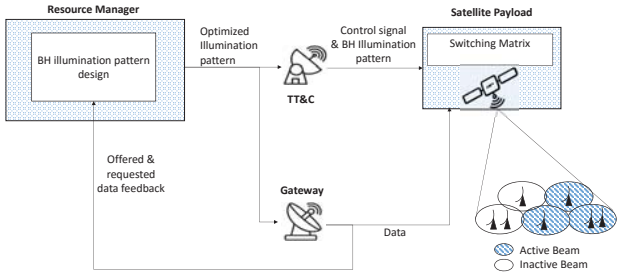

Figure 2. TT&C and Resource Manager in BH system architecture.

Satellite payload designs are becoming increasingly flexible, involving flexible allocation of bandwidth (irregular frequency reuse), of time, and of power. With the emergence of sophisticated payload designs, new satellites, e.g., SES-17 [5], Eutelsat QUANTUM [6], with such flexibility of adapting satellite resources to realistic and dynamic traffic conditions, are expected to be launched in the coming years. BH for satellite systems has been proposed as a promising technological enabler to provide a high level of flexibility to manage irregular and time-variant traffic requests in the satellite coverage area [4], [7]. With BH, all the available satellite resources are employed to provide service to a certain subset of beams, which is active for some portion of time, dwelling just long enough to fill the demand in each beam. The set of illuminated beams changes in each time-slot based on a time-space transmission pattern (called *BH illumination pattern*) that is periodically repeated. Regarding the BH architecture, the most important component is the satellite resource manager, which is the entity that determines the BH illumination pattern. The satellite is informed about the BH illumination pattern via telemetry, tracking, and command (TT&C). A simplified architecture is depicted in Fig. 2, where the TT&C is co-located with the resource management unit. The resource manager is responsible of generating the appropriate illumination pattern that matches the capacity demand, and the outcome is communicated to the satellite gateway and to the payload. The switching matrix in the satellite payload represents the switching capabilities of the payload, which determines the active beams.

B. RELATED WORKS

The challenging task in BH systems is to *determine the beam illumination pattern*, i.e., the beams to be simultaneously activated and for how long. Some studies in the literature have addressed the beam illumination pattern design from different perspectives. Some of the works, e.g., [8]–[10], emerged as a result of the European Space Agency (ESA) project entitled "Beam Hopping Techniques for Multibeam Satellite Systems". In [8], the authors proposed an iterative algorithm for the joint BH time-plan design and the spectrum assignment targeting the maximization of the overall offered capacity of the system subject to certain beam demand and power constraints. Similarly, [9] proposed a heuristic iterative algorithm to find a solution of the BH illumination design. In [10], the goal is to optimize both power and BH design such that the amount of offered capacity is maximized while minimizing the power consumption. The problem cannot be solve optimally, and heuristic solutions based on iterative algorithms are proposed. In [11], the benefits of BH in terms of system performance are analyzed. More precisely, the design of the BH illumination pattern is obtained with genetic algorithms targeting global optimal solution for the system capacity maximization problem. Likewise, the recent work presented in [12] targets the optimal design by making use of the simulated annealing algorithm.

The main difficulty in BH pattern design is the large search space for identifying the optimal patterns. That is, in order to find the optimal solution, the number of possible BH patterns to be searched increases exponentially with the number of beams [8]. For the satellite systems composed of hundreds/thousands of beams, it renders a complicated optimization procedure with long computation times. The conventional exact/optimal solutions are typically impractical for realistic systems, as computational and storage capabilities can exponentially increase with the systems' scale [7]. Given the inherent difficulty in BH design, the capability of a low-complexity suboptimal solution in timely achieving satisfactory performance is limited [13]. In this context, deep learning (DL) appears as a promising technique that offers an alternative to design optimization algorithms for complex

This work is licensed under a Creative Commons Attribution 4.0 License. For more information, see https://creativecommons.org/licenses/by/4.0/.

This article has been accepted for publication in a future issue of this journal, but has not been fully edited. Content may change prior to final publication. Citation information: DOI 10.1109/ACCESS.2020.3011746, IEEE Access

resource management in wireless networks. DL for resource allocation has received considerable research attention over the past few year [14]–[19]. In addition to conventional heuristics, it provides a viable choice in developing efficient solutions. A majority of these works focuses on terrestrial networks, e.g., machine learning techniques in in physical layer communications [14], deep learning for power allocation [15] and scheduling [16], [17], Q-learning for power control [18] and interference control [19].

Combining model-based optimization and data-driven learning techniques for BH pattern design in order to reap maximum benefits from both is an open research issue thus calls for further investigations. In the literature, learning based solutions for satellite BH pattern design, along with their performance evaluation are studied to a limited extent, compared to the learning applications in terrestrial communication systems. A recent work [20] has applied model-free reinforcement learning approaches to optimize BH illumination, where the optimal policy is hardly approached due to the exponentially increased action sets and the inherent suboptimality in such model-free approaches. In general, adopting conventional optimal/suboptimal algorithms for BH optimization would require long computing time to iteratively achieve optimality or near-optimality. Conventional *end-to-end learning (ETEL)*, i.e., relying on a learning model to directly output a complete solution for the addressed optimization problem, may result in solution infeasibility and performance deterioration. This is because, in practice, DL techniques cannot guarantee a perfect prediction, i.e., with 100% accuracy. If one relies on ETEL to directly predict the optimization variables, any inaccurate prediction can possibly violate some constraints or lead to a degraded suboptimal decision.

C. CONTRIBUTIONS

The main contributions of this work are summarized as follows.

- By nature, BH design is a difficult constrained optimization problem, the capability of ETEL or optimization approaches in dealing with such complex problem is however limited from different aspects. Being aware of these shortcomings, we explore a viable way to combine learning and optimization methods for BH design.
- We identify a learnable feature for BH, i.e., the cardinality of the optimal beam patterns, which leads to high accuracy in learning-based prediction. In the proposed learning-and-optimization (L&O) algorithm, we provide an effective manner to integrate learning and optimization components. As a pre-process step, the learning-based prediction is used to cut off non-optimal BH patterns, then the optimization part can be concentrated on a small set only containing promising BH patterns.
- We carry out performance comparisons among optimal, suboptimal, ETEL, and L&O algorithms in terms of computational time and approximating optimality. Numerical study demonstrates that in L&O, the learning component is capable of dramatically accelerating the procedure of promising BH pattern selection. While the optimization component can guarantee the solution's feasibility and achieve near-optimal performance.

The rest of the paper is organized as follows. Section II presents the system models for satellite systems and BH. Section III formulates the BH optimization problem. Section IV characterizes the problems' property and proposes the L&O algorithm. Numerical results are demonstrated in Section V. Conclusions are given in Section VI.

II. SYSTEM MODEL

A. MULTIBEAM SATELLITE SYSTEMS

We consider the forward link of a broadband multibeam satellite system that aggressively reuses frequency resources. We consider a bent-pipe transparent geostationary orbit (GEO) satellite architecture, which relays the signal from the gateway to the final receivers. The satellite payload is assume to be equipped with beam switches, allowing to illuminate different beams at a time. Let us assume the forward link transmission of N satellite beams, which are considered to be equal to the number of transmitting elements on the satellite. For the sake of spectral efficiency, we assume that all beams share the same frequency band B. Note that the co-channel inter-beam interference is minimized by solving the BH optimization problem in section III. The optimized solution is prone to avoid simultaneous illumination of adjacent beams. The key notations are summarized in Table 1.

Table 1. Notations

N	number of beams
n	beam index $n = 1, \ldots, N$
B	bandwidth per beam
D_n	requested demand in beam n
T_H	duration of a BH cycle
g	index of snapshots, $g = 1, \ldots, G$
$\mathcal{N}_g$	set of all the active beams in snapshot g
$\mathcal{G}$	set of candidate snapshots, $\lvert\mathcal{G}\rvert = G$
t_g	duration of snapshot g (continuous or discrete)
R_n	offered capacity for beam n
R_{ng}	achievable rate of beam n in snapshot g
$h_{j,n}$	channel gain from the j-th satellite antenna to beam n
p_n	transmit power for beam n

The channel matrix H, which gathers the forward link budget information and phase rotations introduced by the over-the-air propagation. In particular,

$$H = P\hat{H} \tag{1}$$

where the matrix P models the phase variations due to the different propagation paths and its components $[P]_{x,y}$ are defined as,

$$[P]_{x,y} = \begin{cases} e^{j\phi_x} & \text{if } x = y \\ 0 & \text{otherwise,} \end{cases} \tag{2}$$

being ϕ_x a uniform random variable between $-\pi$ and π.

This work is licensed under a Creative Commons Attribution 4.0 License. For more information, see https://creativecommons.org/licenses/by/4.0/.

This article has been accepted for publication in a future issue of this journal, but has not been fully edited. Content may change prior to final publication. Citation information: DOI 10.1109/ACCESS.2020.3011746, IEEE Access

The matrix $\hat{H}$ represents the real CSI contribution, which is determined by the satellite antenna gain, the path loss, the received antenna gain and the noise power. More precisely, the (k, n)-th component of $\hat{H}$ is given by,

$$\left[\hat{H}\right]_{k,n} = \frac{\sqrt{G_R G_{k,n}}}{4\pi \frac{d_k}{\lambda}\sqrt{K_B T B}} \tag{3}$$

where G_R is the user terminal antenna gain, $G_{k,n}$ denotes the gain from the n-th satellite antenna towards the k-th user served within the n-th beam and d_k is the slant range between the satellite and the k-th user. The term $\sqrt{K_B T B}$ represents the noise contribution, where K_B is the Boltzmann constant, and T is the receiver noise temperature. The model has been widely adopted in the literature, e.g., [8]–[12]. It is common practice to include the noise contribution into the channel model in order to proceed with the assumption of unit-variance noise.

The received signal at the k-th user located at the n-th beam can be expressed as,

$$y_{k,n} = h_{k,n}^T x + n_{k,n}, \tag{4}$$

where $h_{k,n} \in \mathbb{C}^{N\times 1}$ is the CSI vector corresponding to this particular user, $x \in \mathbb{C}^{N\times 1}$ represents the vector of N symbols and $n_{k,n}$ is the complex Additive White Gaussian Noise (AWGN) at user k of beam n. Note that in this paper, we assume an ideal feeder link and lossless processing on-board the satellite. These assumptions allow us to consider x as a signal transmitted from the satellite. Therefore, the channel model considered in this work consists of the forward link (satellite-user link) only.

For the sake of clarity, we can rearrange the received signals (4) by using the following matrix notation,

$$y = Hx + n \tag{5}$$

The received samples are arranged into $y = \begin{bmatrix} y_1^T & \cdots & y_N^T \end{bmatrix}^T$, where y_n is the vector containing the received signal for the users belonging to the n-th beam.

B. BEAM HOPPING

The main design task in BH is to determine which beams to be illuminated together and for how long. The BH illumination pattern design consists of designing a BH cycle of duration T_H, which is periodically repeated. Within a BH cycle, a number of illuminated *snapshots* are used. In this paper, we define a snapshot as a particular arrangement of illuminated and un-illuminated beams. As an example, Fig. 3 illustrates a BH cycle composed of 6 different snapshots. Each beam is covered by the used snapshots at least once. These selected snapshots can be sequentially scheduled with optimized duration.

By enumeration, the total number of possible snapshots, denoted as G, is equal to 2^N, where N is the number of beams. Clearly, the number of snapshots increases exponentially with the number of beams, resulting in a large search space for optimization.

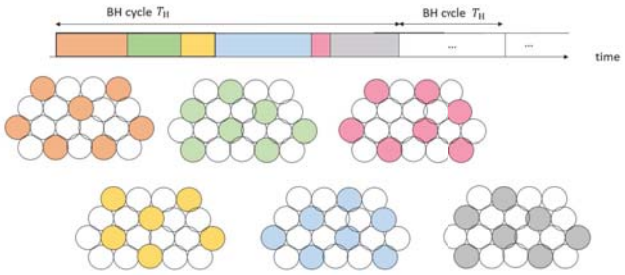

Figure 3. An example of a BH cycle composed of 6 different snapshots.

Remark In this work, we consider a general snapshot set $\mathcal{G}$, and focus on investigating the optimal BH illumination pattern with flexible configuration of snapshots. In practice, the selection of candidate feasible snapshots could be constrained by practical requirements, e.g., minimum SINR requirement, that is, the candidate set $\mathcal{G}$ only contains the snapshots that the SINR in all the active beams is higher than the minimum SINR threshold. This issue can be addressed by pre-processing set $\mathcal{G}$ and excluding those requirement-violated snapshots. □

We define that a BH cycle is segmented into N_{slot} time slots of duration T_{slot} (i.e. $T_H = T_{slot} N_{slot}$). The division of the BH cycle into time-slots is depicted in Fig. 4, where the selected snapshots and its duration are illustrated using different colors. We use variables $t_1, \ldots, t_g, \ldots, t_G$ to represents the number of slots allocated to snapshots $1, \ldots, g, \ldots, G$, respectively. If t_g is equal to 0, then the g-th snapshot is not used. Since each time slot can only be used by at most one snapshot, thus $\sum_{g\in\mathcal{G}} t_g T_{slot} = T_H$.

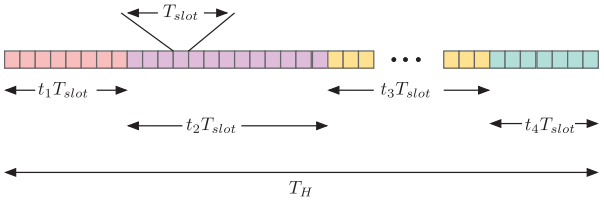

Figure 4. A BH Frame.

A beam can provide service to multiple terminal users in the coverage area. In each beam, multiple terminal users are assumed to be served by the time division multiple access approach [12]. In this paper, we focus on the long-term BH performance at the beam level, and thus, we use beam's demand D_n (equivalent to the case of a single user per beam) to represent the aggregated users' demands in the n-th beam. Then, the channel matrix H can be simplified to a $N \times N$ matrix, where the diagonal elements $h_{n,n}$ represent the channel gain from the n-th satellite antenna to the user in beam n.

This work is licensed under a Creative Commons Attribution 4.0 License. For more information, see https://creativecommons.org/licenses/by/4.0/.

This article has been accepted for publication in a future issue of this journal, but has not been fully edited. Content may change prior to final publication. Citation information: DOI 10.1109/ACCESS.2020.3011746, IEEE Access

$$\boldsymbol{H} = \begin{bmatrix} h_{1,1} & \cdots & h_{1,N} \\ \vdots & \ddots & \vdots \\ h_{N,1} & \cdots & h_{N,N} \end{bmatrix}. \quad (6)$$

The delivered data rate of beam n in snapshot g in a time slot can be expressed as,

$$R_{ng} = T_{slot} B f_{DVB}\left(\frac{p_n h_{n,n}}{\sum_{j\in\mathcal{N}_g\setminus\{n\}} p_j h_{jn} + \sigma^2}\right), \quad (7)$$

where f_{DVB} is the rate mapping function according to the digital video broadcasting through satellite second generation specifications extensions (DVB-S2X) [12]. Note that beam power p_n is treated as fixed parameters. This is because that, in this work, we focus on investigating the performance improvement via exploring time-domain flexibility (by BH pattern optimization), thus other aspects, e.g., power/frequency-domain flexibility, are fixed to facilitate analysis and performance benchmarking.

III. PROBLEM FORMULATION

The considered BH design problem is formulated in P0. The problem aims at optimizing the performance of offered capacity to requested demand ratio (OCDR), i.e., the fraction of the offered capacity (R_n) divided by the requested demand (D_n) of the worst beam, such that the offered and requested capacity can achieve a good match among beams, and the fairness among beams/users can be guaranteed via the max-min operator.

The optimization task is to determine which snapshots to be scheduled in a BH cycle, and how many time slots to be used for each snapshot. The constraint (8b) states that the total duration for the illuminated snapshots should be equal to a BH cycle T_H. Constraints (8c) define the offered capacity for each beam. In (8d), the optimization variables $t_1, \ldots, t_G$ are integer, resulting in a mixed integer linear programming problem (MILP) in P0.

$$\text{P0:} \quad \max_{t_1,\ldots,t_G} \min \left(\frac{R_1}{D_1}, \ldots, \frac{R_N}{D_N}\right) \quad (8a)$$

$$\text{s.t.} \sum_{g\in\mathcal{G}} t_g T_{slot} = T_H, \quad (8b)$$

$$R_n = \sum_{g\in\mathcal{G}} t_g T_{slot} B f_{DVB}\left(\frac{p_n h_{n,n}}{\sum_{j\in\mathcal{N}_g\setminus\{n\}} p_j h_{jn} + \sigma^2}\right), \forall n \quad (8c)$$

$$t_1, \ldots, t_G, \text{ integer} \quad (8d)$$

Solving P0 is difficult in general, in particular for the large-scale instances. The high computational complexity and long computing time impose obstacles for real-time BH scheduling. We circumvent this issue by solving P0's linear relaxation problem which is formulated in P1 with non-negative continuous variables $t_1, \ldots, t_G$ representing the duration of snapshots $1, \ldots, G$, respectively.

$$\text{P1:} \quad \max_{t_1,\ldots,t_G} \min \left(\frac{R_1}{D_1}, \ldots, \frac{R_N}{D_N}\right) \quad (9a)$$

$$\text{s.t.} \sum_{g\in\mathcal{G}} t_g = T_H, \quad (9b)$$

$$R_n = \sum_{g\in\mathcal{G}} t_g B f_{DVB}\left(\frac{p_n h_{n,n}}{\sum_{j\in\mathcal{N}_g\setminus\{n\}} p_j h_{jn} + \sigma^2}\right), \forall n \quad (9c)$$

$$t_1, \ldots, t_G \geq 0. \quad (9d)$$

P1 can be equivalently reformulated as P1' by introducing an auxiliary variable η. From P1', one can observe that P1 is a Linear Programming (LP) problem.

$$\text{P1':} \quad \max_{t_1,\ldots,t_G} \eta \quad (10a)$$

$$\text{s.t.} (9b),\ (9c),\ (9d) \quad (10b)$$

$$\frac{R_n}{D_n} \geq \eta, \forall n = 1, \ldots, N, \quad (10c)$$

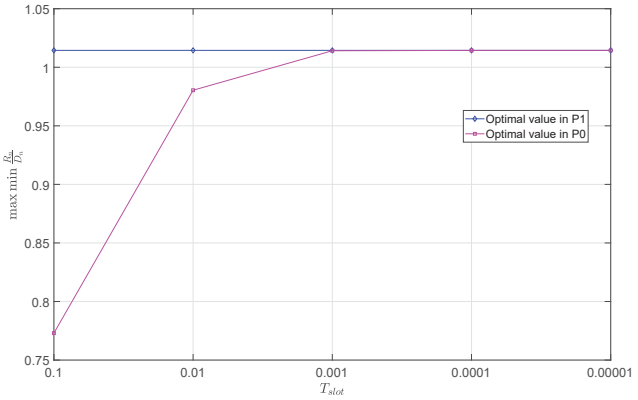

Figure 5. The reduced optimality gaps between P1 and P0 with respect to T_{slot} (in second), 16-beam BH, $T_H = 256\ ms$, average performance over 1000 instances, with the same parameter settings in Section V.

In general, P1 (or P1') provides an upper bound for P0. However, the optimal solution of the LP P1 can ultimately approach to the MILP P0, when the granularity of time slots improves, e.g., reduce the duration T_{slot}. We show this fact by an illustrative example in Fig. 5. We remark that, in ideal cases, OCDR is one which means that the offered capacity perfectly fits the request. In Fig. 5, the optimal ratio is larger than one, which means that in average, the adopted traffic demand among beams maintains at low levels, and the offered capacity is more than the demanded data, referring to as a cold-beam scenario. Once T_{slot} is small enough, e.g., $T_{slot} = 1\ ms$ $(0.001\ s)$, P0 and P1 converge to almost the same optimum points, i.e., with the same objective value and snapshots. As a matter of fact, the time scale T_{slot} of interest in practical satellite BH is in millisecond levels

This work is licensed under a Creative Commons Attribution 4.0 License. For more information, see https://creativecommons.org/licenses/by/4.0/.

This article has been accepted for publication in a future issue of this journal, but has not been fully edited. Content may change prior to final publication. Citation information: DOI 10.1109/ACCESS.2020.3011746, IEEE Access

which provides a fine granularity of T_{slot} and thus good approximation performance. Therefore, under the adopted time scale $T_{slot} = 1\ ms$ which is comparable to the DVB-S2X superframe duration [12], the optimality gap between P0 and P1 can be neglected, and their optimum can be used interchangeably. By doing so, the training data in the proposed L&O algorithm can be generated more efficiently by solving P1 instead of solving P0.

To optimally solve P0 and P1, some standard optimization methods can be applied, e.g., branch-and-bound (B&B) algorithm for MILP P0, and simplex algorithm (SA) or column generation (CG) algorithm for LP P1 [21]. The difficulties come from two aspects. Firstly, the size of candidate snapshot set $\mathcal{G}$ or number of variables in P0 and P1 increase exponentially with the number of beams, e.g., 2^N snapshots in $\mathcal{G}$. When larger-scale scenarios are considered, e.g., more beams, the number of variables in optimization problems P0 and P1 is huge. As a result, the computational complexity and time are not affordable for practical BH scheduling. Secondly, even P1 is an LP problem, the inherent combinatorial explosion remains, i.e., one has to make exponentially many discrete decisions that whether a beam appears in an optimal snapshot or not. The computational time increases exponentially with N in all the three iterative optimization algorithms (B&B, SA, and CG). The reason is that the searching strategy in all the three algorithms are conservative because the optimality must be guaranteed. As a consequence, a large amount of computational efforts are consumed on searching those non-optimal candidates, though time-consuming but have to be executed by the algorithm design.

IV. SOLUTION CHARACTERIZATIONS AND THE PROPOSED ALGORITHM

A. ISSUES IN OPTIMIZATION AND ETEL APPROACHES

The high complexity in optimally solving P1 may motivate the development of low-complexity suboptimal solutions which can provide a timely solution but may with poor performance, e.g., greedy or round-robin algorithms [13], whereas adopting sophisticated heuristics to achieve satisfactory performance would require long computing time [21]. From the learning aspect, classical ETEL approaches, may help but typically only be applicable to some limited instances, e.g., a problem with few variables, non-strict constraints or without constraints [2]. However, in P1, the number of optimization variables increases exponentially with the number of beams. This imposes difficulties to learning/training, and thus may largely increase the difficulty in achieving prediction accuracy. Another issue is the solution's feasibility since any inaccurate prediction in ETEL may violate some constraints thus leading to infeasible solutions. Being aware of these shortcomings in optimization and ETEL, we explore a combined method for BH design, in order to reap the benefits from optimization and learning.

B. SOLUTION CHARACTERIZATION AND FEATURE TO BE LEARNED

At the optimum of P1 or P1', the number of scheduled snapshots will be no more than number of constraints [21], [22], i.e., at most $N + 1$ scheduled snapshots at the optimum of P1'. Note that constraint (9c) and (10c) can be merged into one constraint by replacing R_n with (9c). As a result, the optimized vector $[t_1, \ldots, t_g, \ldots, t_G]$ will be sparse, e.g., $N + 1$ positive elements out of $G = 2^N$. Being aware of this property, we design an aggressive strategy to search the optimum, in contrast to the conservative strategies in B&B, SA, and CG. That is, we train a classifier by neural network to identify a small subset of promising snapshots. The promising snapshots mean that they might not necessarily be optimal, but with high probability to appear in the optimal illumination pattern. The benefits of this aggressive strategy are from two aspects. One is that the optimization process can be more concentrated on the identified small subset, and thus accelerates the overall algorithm. The other is that if the optimality losses in the DL-based prediction, the retained promising snapshots is still capable of providing a feasible and near-optimal solution efficiently.

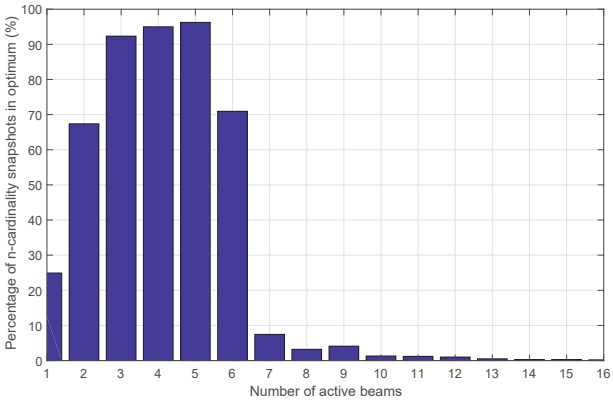

Figure 6. The percentage of scheduling n-cardinality snapshot in optimum (16-beam BH, statistic from the optimal solutions in 10000 realizations, with the same parameter settings in Section V).

From the optimum of P1', the $\max$ operator in the objective is prone to illuminate few beams due to resulting less interference and higher capacity than those large-cardinality snapshots. We illustrate this fact by Fig. 6, where 16-beam BH is adopted and statistic from the optimal snapshots in 10000 realizations. From the figure, the most scheduled snapshots in optimum are concentrated on the snapshots with cardinality 1 to 6. For example, 3-cardinality snapshots are scheduled in about 91% of 10000 instances. In contrast, those large-cardinality snapshots, e.g., 16-cardinality snapshots, are barely scheduled. Based on this observation, we extract the following feature, i.e., the number of simultaneously illuminated beams in optimal snapshots. The feature vector consists of N binary elements, $\boldsymbol{v} = [v_1, \ldots, v_n, \ldots, v_N]$, where v_n represents if any of n-cardinality snapshots (n

This work is licensed under a Creative Commons Attribution 4.0 License. For more information, see https://creativecommons.org/licenses/by/4.0/.

This article has been accepted for publication in a future issue of this journal, but has not been fully edited. Content may change prior to final publication. Citation information: DOI 10.1109/ACCESS.2020.3011746, IEEE Access

active beams in the snapshot) is scheduled in the optimum (v_n = 1), or none of n-cardinality snapshots is used at all (v_n = 0). For example, in 4-beam BH, if the optimal snapshots are $\{\{1,2\},\{1,3,4\},\{2,3\}\}$, the corresponding vector $\boldsymbol{v}$ is $[0,1,1,0]$ since only 2-cardinality and 3-cardinality snapshots are scheduled.

C. THE PROPOSED L&O ALGORITHM

In the proposed L&O algorithm, a training/validation/test set contains two parts, i.e., input parameters and optimal labels. The procedure of data generation is illustrated in Fig. 7. We denote the i-th training/validation/test set as $(\boldsymbol{x}_i, \boldsymbol{v}_i)$. The input $\boldsymbol{x}_i$ is obtained by the i-th realization in emulators, consisting of channel matrix $\boldsymbol{H}$, traffic demand per beam $D_1, \ldots, D_N$, and power per beam $p_1, \ldots, p_N$, where the beam coverage area and $\boldsymbol{H}$ are generated by an adopted satellite emulator. $D_1, \ldots, D_N$ are generated by a recently developed satellite traffic emulator [23]. Note that DL only accepts the real-value inputs, thus the original complex value in $\boldsymbol{H}$ re converted to real values. The optimal labels are organized as feature vector $\boldsymbol{v}_i$ for the i-th realization.

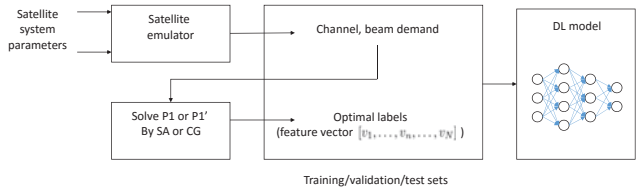

Figure 7. Data generation in training, validation, and testing sets.

A DL model, e.g., fully-connected neural network (FC-NN), is trained to learn the mapping from the input to the optimal label. We summarize the procedure of L&O in Algorithm 1. Taking a test set to the after-trained FC-NN, the model is able to provide a predicted feature vector efficiently [24]. From line 3 to 8, a rounding operation is adopted to convert fractional elements in $\boldsymbol{v}$ to binary, where α is a control parameter. By design, decreasing α results in more "1" elements appearing in $\boldsymbol{v}$. From line 9 to line 11, we form a subset $\mathcal{G}^*$ after deleting a large amount of non-promising snapshots from original set $\mathcal{G}$ by scanning all the "0" elements in $\boldsymbol{v}$. At the last step, the optimized results $t_1^*, \ldots, t_G^*$ can be obtained by optimally solving P1 or P1' with the small subset $\mathcal{G}^*$.

Algorithm 1 L&O for BH Scheduling

1: Generate $(\boldsymbol{x}_i, \boldsymbol{v}_i),\ i = 1, \ldots, I$ and train a DL model
2: Take a test set to DL and obtain a predicted vector $\boldsymbol{v}$
3: $M = \sum_{n=1}^{N} v_n/N,\ v_n \in \boldsymbol{v}$
4: **for** $n = 1, \ldots, N$ **do**
5: **if** $v_n \notin \{0,1\}$ and $v_n > \alpha M$, **then**
6: $v_n = 1$
7: **else**
8: $v_n = 0$
9: **for** $n = 1, \ldots, N$ **do**
10: **if** $v_n = 0$ **then**
11: $\mathcal{G}^* \triangleq \mathcal{G}^* \backslash \{g \in \mathcal{G}^* : |\mathcal{N}_g| = n\}$
12: $\mathcal{G} \leftarrow \mathcal{G}^*$ in P1 or P1'
13: Solve P1 or P1' with $\mathcal{G}^*$ to obtain $t_1^*, \ldots, t_G^*$

V. NUMERICAL RESULTS

A. EXPERIMENTAL SETUP

To evaluate the performance of the proposed L&O algorithm, we adopt a real-life multi-beam GEO scenario. The antenna pattern is provided by ESA in format (latitude, longitude, gain) [26]. We call this scenario "ESA71" consisting of 71 beams in total [25]. The beam pattern and the coverage area of ESA71 are illustrated in Fig. 8. We extract 16 beams out of the ESA 71 beam pattern for the simulations. For traffic-demand generation, we adopt a recently developed

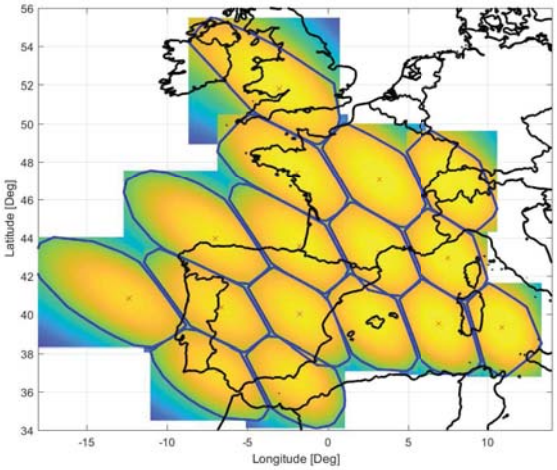

Figure 8. Adopted 16 beams from the ESA71 Beam pattern [25].

traffic emulator [23]. The traffic emulator models the traffic demand distribution over Europe by processing credible datasets included three major input categories of information: Population distribution for broadband Fixed Satellite Services (FSS), aeronautical satellite communications, and vessel distribution for maritime services. This traffic emulator combines these three dimensional information to extract the time domain characteristics of the geographical traffic patterns, and obtain an accurate traffic model over 24 hour time-span.

In terms of training, we firstly perform tests for evaluating several hyper-parameters, e.g., number of hidden layers, neurons per layer, batch size, epochs, activation functions, optimizer, and learning rate, such that the selected parameters are able to lead to overall satisfactory performance for the considered optimization problem. The parameters of the satellite scenario and the adopted FC-NN are summarized in Table 2.

This work is licensed under a Creative Commons Attribution 4.0 License. For more information, see https://creativecommons.org/licenses/by/4.0/.

This article has been accepted for publication in a future issue of this journal, but has not been fully edited. Content may change prior to final publication. Citation information: DOI 10.1109/ACCESS.2020.3011746, IEEE Access

Table 2. Parameter Settings

Satellite System Parameters	Value
Satellite longitude	13^0 (GEO)
Satellite height	35,786 km
Number of beams	16
Carrier frequency	19.5 GHz
Bandwidth per beam	500 MHz
Boltzmann constant	-228.6 dBW/K/Hz
Receiver noise temperature	235.3 K
Transmit power per beam	20 dBW
Receive antenna gain	40.7 dBi
Feed radiation pattern	[26]
Roll-off factor	0.2
BH cycle T_H	256 ms
T_{slot}	1 ms
FC-NN Parameters	**Value**
Number of hidden layers	3
Nodes per hidden layer	200
Nodes at output layer	$N = 16$
Activation function	Relu, Sigmoid
Optimizer	Adam, RMSprop [24]
Loss function	Mean Squared Error (MSE)
Size of training sets	18000
Size of test sets	2000
Batch size	128
Number of epochs	450
L&O implementation	Python + TensorFlow
B&B, SA, and CG	Python + Gurobi

B. PERFORMANCE COMPARISON AMONG L&O, ETEL, SUBOPTIMAL, AND OPTIMAL ALGORITHMS

We demonstrate the performance gain of L&O over conventional optimization algorithms and ETEL, in terms of computational time and approximating optimality. Firstly, in Fig. 9, we compare the computational time (in seconds) of L&O (executing lines 2 to 13 in Algorithm 1) with other four benchmaking algorithms, i.e., the optimal B&B algorithm for solving the integer problem P0, the optimal SA and CG algorithms for solving the LP problem P1, a low-complexity suboptimal approach used in [27], and the conventional ETEL learning approach. To implement the approach in [27], two beams who have received the least interference are activated simultaneously, and the time allocation among illumination patterns is proportional to their traffic demand.

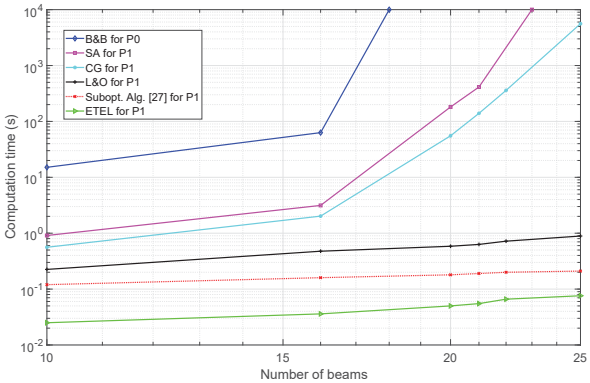

Figure 9. Computational time comparison among optimal, suboptimal, ETEL, and L&O algorithms

Each value in Fig. 9 is averaged by 1000 test sets. The time is recorded from giving a new test set to the algorithms until they return the optimized results. The time consumption in B&B, SA, and CG exponentially increases with the number of beams, whereas the other three algorithms increase moderately. The average computational time in L&O is slightly higher than ETEL and the heuristic approach in [27], but has reduced to within one second, and is insensitive to the problem's scale. The reason is that NN is computationally light [24] by its nature, thus ETEL yields the minimum computational time. The heuristic approach in [27] adopts simple design to guarantee its computational efficiency in resource management, thus is more efficient than L&O. The FC-NN in L&O takes advantages from efficient learning. We remark that the majority of computational time in L&O is consumed at solving the restricted problem. However, by using the predicted results from FC-NN, we keep the restricted set small to enable a much more efficient solution than B&B, SA, and CG with the original set. For example, the restricted set in L&O only contains hundreds of variables/snapshots (promising to be optimal) in average. In comparison, the original set in B&B, SA, CG has 2^{16} variables to be optimized thus is time consuming. Combining with the demonstrated OCDR value in Fig. 10, L&O can achieve better trade-off than other algorithms. That is, when the FC-NN in L&O is sufficiently trained, L&O is near-optimal, 5% lower than the optimum but it saves numerous computational time, e.g., see OCDR at 9000 training data sets and time in Fig. 9. On the other hand, L&O consumes slightly more time than the heuristic approach in [27], but brings significant performance gain in improving OCDR.

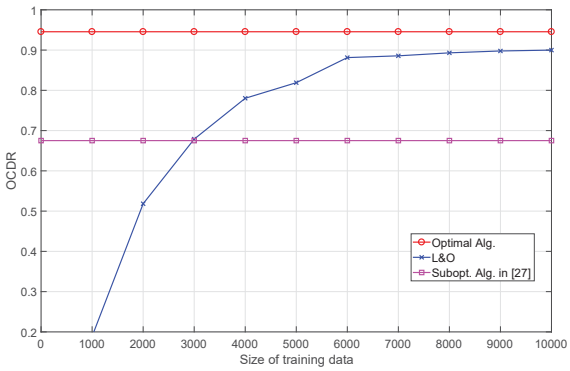

Figure 10. OCDR performance comparison among optimal, suboptimal, and L&O algorithms.

Next, Fig. 11 shows the performance of L&O in approximating optimality, which can be used to explain the achieved near-optimality of L&O. The metric "accuracy" presents the ratio of how many elements in the predicted feature vector $\boldsymbol{v}$ consistent with the optimum. For example, "0.8" means that in average 80% predicted elements in $v_1, \ldots, v_N$ hit the optimum. In general, high ratio leads to near-optimal performance. From the results, the average accuracy ratio maintains around 95% when the training sets are sufficient.

This work is licensed under a Creative Commons Attribution 4.0 License. For more information, see https://creativecommons.org/licenses/by/4.0/.

This article has been accepted for publication in a future issue of this journal, but has not been fully edited. Content may change prior to final publication. Citation information: DOI 10.1109/ACCESS.2020.3011746, IEEE Access

This also implies that the designed feature is appropriate and learnable, also referring to the reason explained in Fig. 6. Benefiting by this high accuracy, the OCDR values between L&O and the optimum are close.

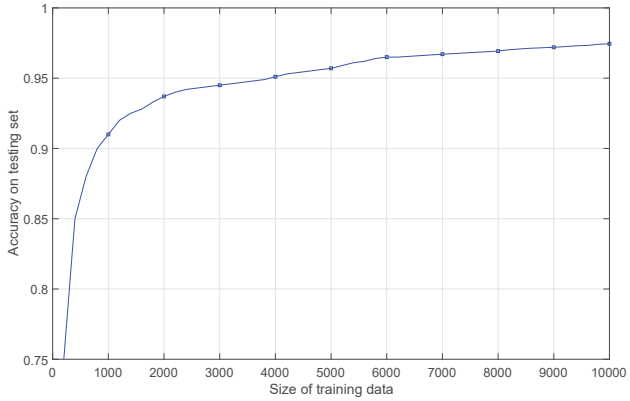

Figure 11. The ratio of hitting optimality with respect to training set size (activation function: Rectified Linear Unit (ReLU), optimizer: Adaptive Moment Estimation (Adam)).

In contrast, we use an illustrative example in Fig. 12 to show the performance of ETEL. The same FC-NN is adopted except that it learns then outputs predicted $t_1, \ldots, t_G$ instead of $v_1, \ldots, v_N$. The optimal OCDR and ETEL are compared and demonstrated in 500 test sets. From the results, the solutions derived by ETEL are infeasible in almost all the instances due to the imperfect prediction in FC-NN and the resulting constraint violations. In addition, the optimality gaps are considerably large, merely achieving less than 50% of the optimal OCDR in average. This is because the large amount of nodes in the output layer introduces more difficulties for the learning task. When more hidden layers and more training data sets are adopted, the performance improvement of ETEL is marginal. Therefore, an appropriate learning feature is critical for the overall performance. Applying DL to directly predict variables $t_1, \ldots, t_G$, though straightforward, but may not be a wise choice for the BH scheduling problem. The results also confirm the necessity of designing learnable features.

C. PERFORMANCE OF FC-NN IN L&O

The FC-NN lies in the core component of L&O which significantly influences the overall L&O performance. Next, we thoroughly evaluate the FC-NN performance under various hyper-parameters, in terms of accuracy and loss.

1) Performance with Respect to α

In Fig. 13, we show that the accuracy performance of FC-NN and the computational time of L&O can be scaled by the control parameter α. In general, smaller α rounds more fractional elements to "1" for the predicted vector $\boldsymbol{v}$. On the one hand, this can retain more snapshots/variables in the

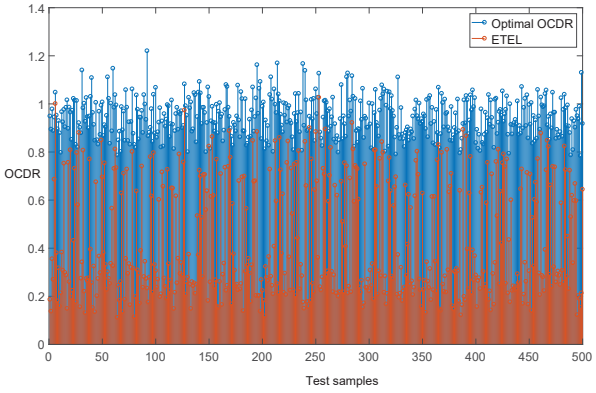

Figure 12. Performance of ETEL (training set size 10000, 5 hidden layers, activation function: ReLU, optimizer: Adam).

restricted set. The scale of subset $\mathcal{G}^*$ grows due to more "1" elements in $\boldsymbol{v}$. Thus, the complexity of L&O will increase correspondingly, referring to the computational time in Fig. 13 with respect to α. On the other hand, larger subset $\mathcal{G}^*$ can accommodate more promising snapshots thus achieves better performance than smaller $\mathcal{G}^*$. In contrast, higher threshold excludes more snapshots out of the restricted set. Then fewer variables typically leads to lower complexity but it also brings larger optimality loss since some optimal candidates might be wrongly filtered. In practice, scaling α can be used as an effective and simple way to trade off the near optimality and complexity.

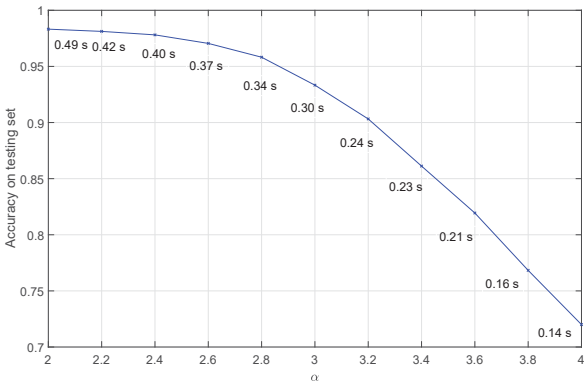

Figure 13. Predict accuracy and computational time with respect to parameter α (activation function: ReLU, optimizer: Adam).

2) Performance with Respect to Hidden Layers

In Fig. 14, we investigate the accuracy performance with respect to number of hidden layers. By adopting ReLU and Sigmoid as the activation function, the accuracy in Sigmoid instances achieves the best at 2 hidden layers. More hidden layers may not necessarily lead to better performance when the size of the used training sets remains, e.g., see the performance degeneration for more than 8 hidden layers. In

This work is licensed under a Creative Commons Attribution 4.0 License. For more information, see https://creativecommons.org/licenses/by/4.0/.

This article has been accepted for publication in a future issue of this journal, but has not been fully edited. Content may change prior to final publication. Citation information: DOI 10.1109/ACCESS.2020.3011746, IEEE Access

ReLU, the best accuracy achieves at the 4-layer cases. When more hidden layers are adopted in FC-NN, the performance maintains but the improvement becomes marginal.

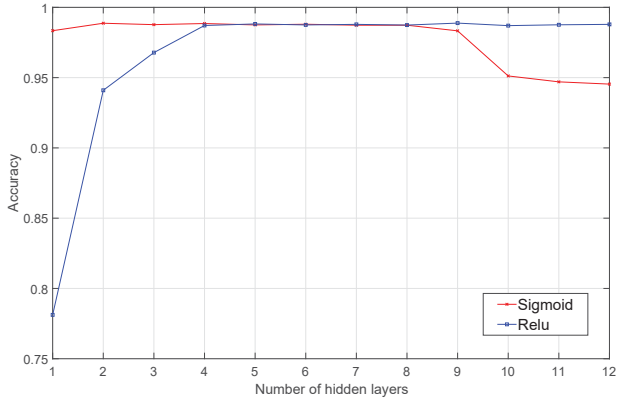

Figure 14. Predict accuracy with respect to number of hidden layers (optimizer: Adam).

3) Performance with Respect to Neurons Per Layer

In Fig. 15, we investigate the accuracy performance with respect to number of neurons per hidden layer. By adopting ReLU (the performance behavior of Sigmoid is consistent with the performance of ReLU) and Adam, the accuracy improvement is considerable from 5-nodes to 100-nodes per layer. When more nodes are introduced to each hidden layer, the accuracy improvement becomes marginal.

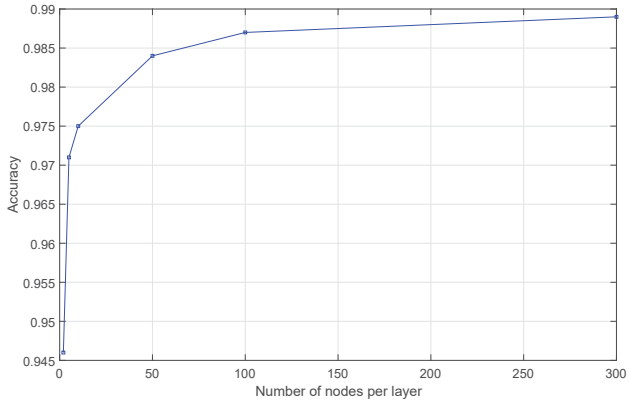

Figure 15. Predict accuracy with respect to number of neurons per layer (optimizer: Adam, activation function: ReLU, 3 hidden layers).

4) Impact of Optimizer and Activation Function on Loss Convergence

Next, we investigate an important performance metric, convergence of the loss value. In FC-NN training, we essentially minimize a loss function (or referred to as simply loss). The goal is to find a set of weight values such that the loss is minimized. The loss value provides a measure for the performance of FC-NN training on a given data set. In Fig. 16, we evaluate the combinations of the two widely used DL optimizer, Adam and Root Mean Square Propagation (RMSprop), with two activation functions, ReLU and Sigmoid, in training and test sets. The convergence of the loss value is related to the choice of the activation function [24]. In Fig. 16(a) and Fig. 16(b), ReLU is adopted the activation function in FC-NN, then in Fig. 16(c) and Fig. 16(d), we further investigate Sigmoid in training and test sets. In general, by adopting Adam or RMSprop, and ReLU or Sigmoid, the FC-NN training is successful. The performance of Sigmoid is slightly better than ReLU in terms of the lower loss. The combination of RMSprop and ReLU has the highest efficiency in reducing loss, see the sharp drop before 10^4 iterations. The performance in training sets is consistent with the test sets, which means no over-fitting or under-fitting effect on the data sets.

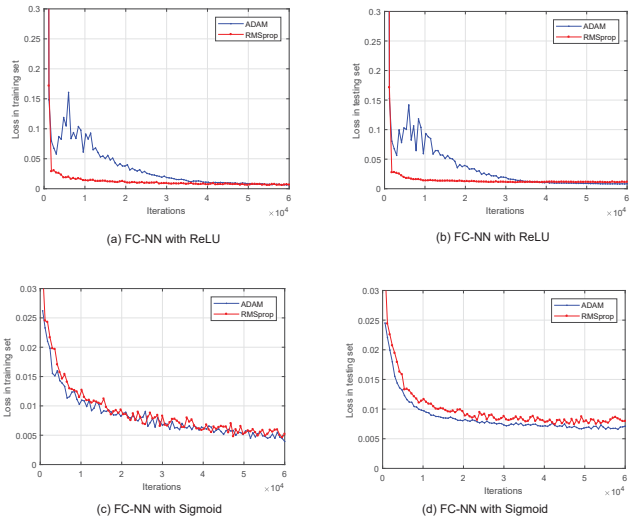

Figure 16. Convergence of loss value in training and testing sets, using activation function ReLU in (a), (b), and Sigmoid in (c), (d).

5) Impact of Optimizer and Activation Function on Accuracy

In terms of the accuracy in FC-NN, we evaluate the performance impact by adopting Adam, RMSprop, ReLU, and Sigmoid. The results on test sets are shown in Fig. 17. After sufficient training, the predict accuracy is high in both figures. Around 95% of the elements in the predicted $\boldsymbol{v}$ are as same as the optimal solution. From the results, the combinations RMSProp-ReLU or Adam-Sigmoid achieve better performance than Adam-ReLU or RMSProp-Sigmoid, respectively.

6) Impact of Learning Rate on Loss and Accuracy

Next, we evaluate the impact of learning rate on the performance of loss and prediction accuracy. Learning rate (or

This work is licensed under a Creative Commons Attribution 4.0 License. For more information, see https://creativecommons.org/licenses/by/4.0/.

This article has been accepted for publication in a future issue of this journal, but has not been fully edited. Content may change prior to final publication. Citation information: DOI 10.1109/ACCESS.2020.3011746, IEEE Access

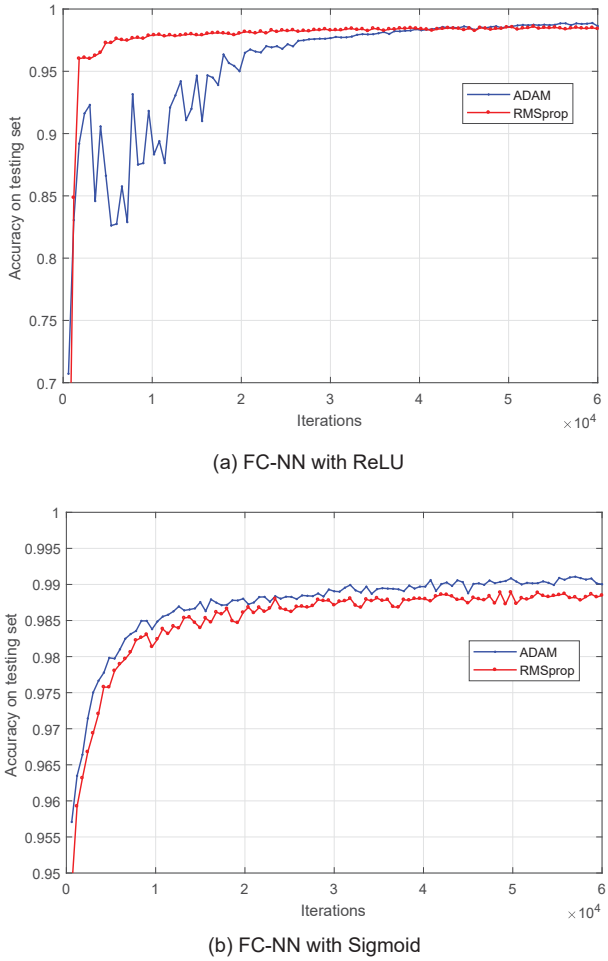

Figure 17. Predict accuracy in FC-NN test sets, using ReLU in (a) and Sigmoid in (b).

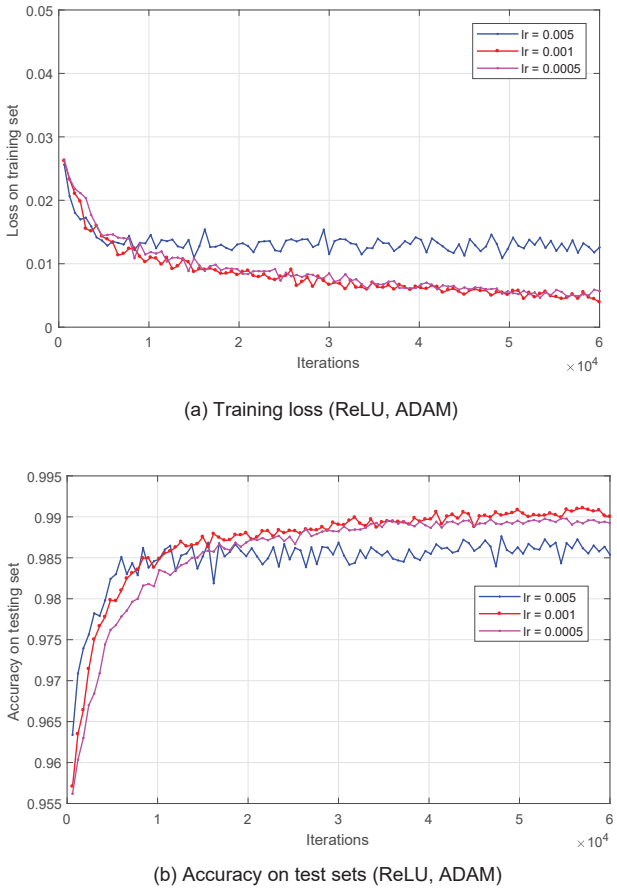

Figure 18. (a) Training loss evolution and (b) Accuracy evolution on test sets with respect to learning rates (ReLU and Adam).

referred to as the step size) is a hyper-parameter in FC-NN training that controls how much the weights are adjusted with respect the loss gradient, often ranging between 0.0 and 1.0. Selecting the learning rate is challenging in training FC-NN. It is considered as one of the most important hyper-parameters for the DL model. If the learning rate is too large, it may result in learning a sub-optimal set of weights too fast or an unstable training process, whereas the small learning rate may lead to long training process. From Fig.18, the learning rate should be carefully selected in order to achieve better performance. From the results, the learning rate 0.001 yields the best performance in both figures. The performance is degraded when either large or small learning rates are adopted.

VI. CONCLUSION

In this paper, we have investigated the problem of efficient BH illumination pattern design. The proposed L&O algorithm has combined the benefits of learning techniques and optimization approaches. For applying learning techniques to solve the problem, we have showed that it is of importance to learn the proper features in order to come up with a good prediction. Numerical results have showed that FC-NN can be used to limit the search space of optimization problems, and therefore speed-up the process of obtaining feasible, efficient, and near-optimal solutions. In this way, the efficient computations of FC-NN is combined with the high-quality and feasible solution of the optimization approach.

References

[1] O. Simeone, "A Very Brief Introduction to Machine Learning With Applications to Communication Systems," in IEEE Transactions on Cognitive Communications and Networking, vol. 4, no. 4, pp. 648–664, Dec. 2018.

[2] M. Chen, U. Challita, W. Saad, C. Yin and M. Debbah, "Artificial Neural Networks-Based Machine Learning for Wireless Networks: A Tutorial," in IEEE Communications Surveys & Tutorials, pre-print, 2019.

[3] Z. Chang, L. Lei, Z. Zhou, S. Mao, and T. Ristaniemi, "Learn to Cache: Machine Learning for Network Edge Caching in the Big Data Era," IEEE Wireless Communications, vol. 25, no. 3, pp. 28–35, Jun. 2018.

[4] J. Anzalchi, et al., "Beam Hopping in Multi-Beam Broadband Satellite Systems: System Simulation and Performance Comparison with Non-Hopped Systems," in proc. Advanced Satellite Multimedia Systems Conference (ASMS), pp. 248–255, Sept. 2010.

[5] SES-17, "SES first flexible satellite," https://www.ses.com/press-

This work is licensed under a Creative Commons Attribution 4.0 License. For more information, see https://creativecommons.org/licenses/by/4.0/.

This article has been accepted for publication in a future issue of this journal, but has not been fully edited. Content may change prior to final publication. Citation information: DOI 10.1109/ACCESS.2020.3011746, IEEE Access

release/ses-and-thales-unveil-next-generation-capabilities-onboard-ses-17.

[6] EUTELSAT QUANTUM, "EUTELSAT first flexible satellite," https://www.eutelsat.com/fr/satellites/futurs-satellites/Eutelsat-Quantum.html.

[7] A. Freedman, D. Rainish, and Y. Gat, "Beam Hopping: How To Make it Possible," in proc. Ka and Broadband Communication Conference, Oct. 2015.

[8] J. Lei and M. Vazquez-Castro, "Multibeam Satellite Frequency/Time Duality Study and Capacity Optimization," in proc. IEEE International Conference on Communications (ICC), vol. 13, no. 5, pp. 471–480, Oct. 2011.

[9] X. Alberti, et al., "System Capacity Optimization in Time and Frequency for Multibeam Multi-Media Satellite Systems," in proc. Advanced Satellite Multimedia Systems Conference (ASMS), pp. 226–233, Sept. 2010.

[10] R. Alegre-Godoy, N. Alagha, and M. Vazquez-Castro, "Offered Capacity Optimization Mechanisms for Multibeam Satellite Systems," in proc. IEEE International Conference on Communications (ICC), Jun. 2012.

[11] P. Angeletti, D. Fernandez-Prim, and R. Rinaldo, "Beam Hopping in Multi-Beam Broadband Satellite Systems: System Performance and Payload Architecture Analysis," in proc. AIAA International Communications Satellite Systems Conference (ICSSC), Jun. 2006.

[12] G. Cocco, T. de Cola, M. Angelone, Z. Katona, and S. Erl, "Radio Resource Management Optimization of Flexible Satellite Payloads for DVB-S2 Systems," in IEEE Transactions on Broadcasting, vol. 64, no. 2, pp. 266–280, Jun. 2018.

[13] F. Calabrese, L. Wang, E. Ghadimi, G. Peters, L. Hanzo, and P. Soldati, "Learning Radio Resource Management in RANs: Framework, Opportunities, and Challenges," in IEEE Communications Magazine, vol. 56, no. 9, pp. 138–145, Sept. 2018.

[14] T. O'Shea and J. Hoydis, "An Introduction to Deep Learning for the Physical Layer," in IEEE Transactions on Cognitive Communications and Networking, Dec. 2017.

[15] H. Sun, X. Chen, Q. Shi, M. Hong, X. Fu, and N. Sidiropoulos, "Learning to Optimize: Training Deep Neural Networks for Wireless Resource Management," IEEE International Workshop on Signal Processing Advances in Wireless Communications (SPAWC), pp. 1–6, Jul. 2017.

[16] L. Lei et al., "Learning-Assisted Optimization for Energy-Efficient Scheduling in Deadline-Aware NOMA Systems," in IEEE Transactions on Green Communications and Networking, vol. 3, no. 3, pp. 615-627, Sept. 2019.

[17] L. Lei, L. You, G. Dai, T. Vu, D. Yuan, and S. Chatzinotas, "A Deep Learning Approach for Optimizing Content Delivering in Cache-Enabled HetNet," in proc. IEEE International Symposium on Wireless Communication Systems (ISWCS), Aug. 2017.

[18] E. Ghadimi, F. Calabrese, G. Peters, and P. Soldati, "A Reinforcement Learning Approach to Power Control and Rate Adaptation in Cellular Networks," in proc. IEEE International Conference on Communications (ICC), May 2017.

[19] M. Bennis and D. Niyato, "A Q-learning Based Approach to Interference Avoidance in Self-Organized Femtocell Networks," in proc. IEEE Globecom Workshops, Dec. 2010.

[20] X. Hu, Y. Zhang, X. Liao, Z. Liu, W. Wang and F. M. Ghannouchi, "Dynamic Beam Hopping Method Based on Multi-Objective Deep Reinforcement Learning for Next Generation Satellite Broadband Systems," in IEEE Transactions on Broadcasting, pre-print, 2019.

[21] K. Murty, Linear programming. NJ, USA: Wiley, 1983.

[22] L. Lei, D. Yuan, C. K. Ho, and S. Sun, "Optimal cell clustering and activation for energy saving in load-coupled wireless networks," in IEEE Transactions on Wireless Communications, vol. 14, no. 11, pp. 6150–6163, Nov. 2015.

[23] "SnT SIGCOM Satellite Traffic Emulator," online: https://wwwfr.uni.lu/snt/research/sigcom/sw-simulators/.

[24] I. Goodfellow, Y. Bengio, and A. Courville, Deep Learning. London, UK: MIT Press, 2016.

[25] "ESA Project FlexPreDem - Demostrator of Precoding Techniques for Flexible Broadband Systems," online: https://artes.esa.int/projects/flexpredem.

[26] ESA, "SATellite Network of EXperts (SATNEX) IV," https://satnex4. org/.

[27] A. Ginesi, E. Re, and P. Arapoglou, "Joint Beam Hopping and Precoding in HTS Systems", in proc. International Conference on Wireless and Satellite Systems (WiSATS), pp 43-51, 2017.

LEI LEI (S'12-M'17) is currently a Research Scientist at the Interdisciplinary Centre for Security, Reliability and Trust (SnT), University of Luxembourg. He received the B.Eng. and M.Eng. degrees from Northwestern Polytechnic University, Xi'an, China, in 2008 and 2011, respectively. He obtained his Ph.D. degree in 2016 at the Department of Science and Technology, Linköping University, Sweden. He joined SnT as a research associate in Nov. 2016. He was a research assistant at Institute for Infocomm Research (I2R), A*STAR, Singapore, from June 2013 to December 2013. His current research interests include resource allocation and optimization in 5G-satellite networks, energy-efficient communications, and deep learning in wireless communications. He received the IEEE Sweden Vehicular Technology-Communications-Information Theory (VT-COM-IT) joint chapter best student journal paper award in 2014. He was a co-recipient of the IEEE SigTelCom 2019 Best Paper Award.

EVA LAGUNAS (S'09-M'13-SM'18) received the M.Sc. and Ph.D. degrees in telecommunications engineering from the Polytechnic University of Catalonia (UPC), Barcelona, Spain, in 2010 and 2014, respectively. She was Research Assistant within the Department of Signal Theory and Communications, UPC, from 2009 to 2013. During the summer of 2009 she was a guest research assistant within the Department of Information Engineering, Pisa, Italy. From November 2011 to May 2012 she held a visiting research appointment at the Center for Advanced Communications (CAC), Villanova University, PA, USA. In 2014, she joined the Interdisciplinary Centre for Security, Reliability and Trust (SnT), University of Luxembourg, where she currently holds a Research Scientist position. Her research interests include radio resource management and general wireless networks optimization.

YAXIONG YUAN (S'18) received the M.S. degree from the Laboratory of Wireless Communication Systems and Networks (WCSN), Beijing University of Posts and Telecommunications, Beijing, China. He is currently pursuing the Ph.D degree with Interdisciplinary Centre for Security, Reliability and Trust, University of Luxembourg, Luxembourg. His research interests include wireless communication, focusing on wireless resource management based on optimization theory and machine learning.

This work is licensed under a Creative Commons Attribution 4.0 License. For more information, see https://creativecommons.org/licenses/by/4.0/.

This article has been accepted for publication in a future issue of this journal, but has not been fully edited. Content may change prior to final publication. Citation information: DOI 10.1109/ACCESS.2020.3011746, IEEE Access

MIRZA GOLAM KIBRIA (S'11–M'14) received the B.E. degree from Visveswaraiah Technological University, India, in 2005, the M.Sc. degree from the Lund Institute of Technology, Lund University, Sweden, in 2010, and the Ph.D. degree from Kyoto University, Japan, in 2014, all in electrical engineering. In 2014, he joined the National Institute of Information and Communications Technology, where he was a Researcher with the Wireless Systems Laboratory, Wireless Network Research Center, Yokosuka Research Park, Japan. Since September 2018, he is with SIGCOM, SnT, University of Luxembourg, Luxembourg. His research interests include resource allocation optimization, wireless signal processing, shared spectrum access communications, small cell networks, and stochastic geometry. He was a recipient of the Japanese Government (Monbukagakusho, formerly known as Monbusho) Scholarship for his Ph.D. study. He was a recipient of the IEICE WBS Student Paper Award in 2013, the IEEE WPMC Best Paper Award in 2015, and the Young Researcher's Encouragement Award from the Japan chapter of the IEEE Vehicular Technology Society in 2012.

SYMEON CHATZINOTAS (S'06–M'09–SM'13) is currently Full Professor / Chief Scientist I and Co-Head of the SIGCOM Research Group at SnT, University of Luxembourg. In the past, he has been a Visiting Professor at the University of Parma, Italy and he was involved in numerous Research and Development projects for the National Center for Scientific Research Demokritos, the Center of Research and Technology Hellas and the Center of Communication Systems Research, University of Surrey. He received the M.Eng. degree in telecommunications from the Aristotle University of Thessaloniki, Thessaloniki, Greece, in 2003, and the M.Sc. and Ph.D. degrees in electronic engineering from the University of Surrey, Surrey, U.K., in 2006 and 2009, respectively. He was a co-recipient of the 2014 IEEE Distinguished Contributions to Satellite Communications Award, the CROWNCOM 2015 Best Paper Award and the 2018 EURASIP JWCN Best Paper Award. He has (co-)authored more than 400 technical papers in refereed international journals, conferences and scientific books. He is currently in the editorial board of the IEEE Open Journal of Vehicular Technology and the International Journal of Satellite Communications and Networking.

BJÖRN OTTERSTEN (S'87–M'89–SM'99–F'04) was born in Stockholm, Sweden, in 1961. He received the M.S. degree in electrical engineering and applied physics from Linköping University, Linköping, Sweden, in 1986, and the Ph.D. degree in electrical engineering from Stanford University, Stanford, CA, USA, in 1990. He has held research positions with the Department of Electrical Engineering, Linköping University, the Information Systems Laboratory, Stanford University, the Katholieke Universiteit Leuven, Leuven, Belgium, and the University of Luxembourg, Luxembourg. From 1996 to 1997, he was the Director of Research with ArrayComm, Inc., a start-up in San Jose, CA, USA, based on his patented technology. In 1991, he was appointed a Professor of signal processing with the Royal Institute of Technology (KTH), Stockholm, Sweden. From 1992 to 2004, he was the Head of the Department for Signals, Sensors, and Systems, KTH, and from 2004 to 2008, he was the Dean of the School of Electrical Engineering, KTH. He is currently the Director for the Interdisciplinary Centre for Security, Reliability and Trust, University of Luxembourg. As Digital Champion of Luxembourg, he acts as an Adviser to the European Commission. He was a recipient of the IEEE Signal Processing Society Technical Achievement Award in 2011 and the European Research Council advanced research grant twice, in 2009–2013 and in 2017–2022. He has co-authored journal papers that received the IEEE Signal Processing Society Best Paper Award in 1993, 2001, 2006, and 2013, and seven other IEEE conference papers best paper awards. He has served as Editor-in-Chief of EURASIP Signal Processing Journal, Associate Editor for the IEEE TRANSACTIONS ON SIGNAL PROCESSING and the Editorial Board of the IEEE Signal Processing Magazine. He is currently a member of the editorial boards of EURASIP Journal of Advances Signal Processing and Foundations and Trends of Signal Processing. He is a fellow of IEEE and EURASIP.

This work is licensed under a Creative Commons Attribution 4.0 License. For more information, see https://creativecommons.org/licenses/by/4.0/.

View publication stats